Excited States of Porphyrin Macrocycles

Laura Moroni, Cristina Gellini, and Pier Remigio Salvi*

Dipartimento di Chimica, Università di Firenze, via della Lastruccia 3, 50019 Sesto Fiorentino, Firenze, Italy

Agnese Marcelli

Laboratorio Europeo di Spettroscopie non Lineari (LENS), Università di Firenze, via N. Carrara 1, 50019 Sesto Fiorentino, Firenze, Italy

Paolo Foggi†

Dipartimento di Chimica, Università di Perugia, via Elce di Sotto 8, 06123 Perugia, Italy

Received: April 15, 2008; Revised Manuscript Received: August 29, 2008

$S_1 \rightarrow S_n$ spectra of porphyrin, diprotonated porphyrin, and tetraoxaporphyrin dication have been measured in the energy range 2−3 eV above S_1 at room temperature in solution by means of transient absorption spectroscopy exciting with femtosecond pulses. Highly excited $\pi\pi^*$ states not active in the conventional $S_0 \rightarrow S_n$ spectrum have been observed. The experimental data are discussed on the basis of the time dependent density functional theory taking advantage of large scale calculations of configuration interaction between singly excited configurations (DF/SCI). The DF/SCI calculation on porphyrin has allowed to assign *g* states active in the $S_1 \rightarrow S_n$ spectrum. Applying the same calculation method to tetraoxaporphyrin dication the $S_0 \rightarrow S_n$ spectrum is reproduced relatively to the Q and B (Soret) bands as well as to the weaker E_u bands at higher energy. According to our calculation the $S_1 \rightarrow S_n$ transient spectrum is related to states of *g* symmetry mainly arising from excitations between doubly degenerate π and π^* orbitals such as $2e_g \rightarrow 4e_g$. In the case of diprotonated porphyrin it is shown that the complex of the macrocycle with two trifluoroacetate anions plays a significant role for absorption. Charge transfer excitations from the anions to the macrocycle contribute to absorption above the Soret band, justifying the intensity enhancement of the $S_0 \rightarrow S_n$ spectrum with respect to the other two macrocyclic systems.

I. Introduction

Due to the role of porphyrins in fundamental biological functions, such as oxygen transport and storage in aerobic organisms[1] and conversion of solar to chemical energy in photosynthetic reaction centers,[2,3] the relaxation dynamics and assignment of porphyrin excited states are issues which have attracted over the years interest in chemical investigations on these macrocycles.[4] Much work was concerned with the characterization of the lowest $\pi\pi^*$ states,[5−13] traditionally denoted as Q_x;Q_y and B_x;B_y in planar D_{2h} porphyrins and Q,B in D_{4h} metalloporphyrins.[5] Recently, results on the primary decay channels from these states following the excitation in the Soret band by femtosecond light pulses have been reported in detail.[14−21] For instance, in tetraphenylporphyrin and unsubstituted porphyrin the (B_x;B_y) → Q_y and Q_y → Q_x internal conversion processes take place in the ultrashort time domain of tens/hundreds of femtoseconds.[14−16] The decay becomes slower in zinc porphyrins owing to the wider energy gap ΔE(B-Q) with respect to porphyrins.[17−19]

On the other hand, $\pi\pi^*$ states of porphyrins higher than the B_x;B_y pair have been also observed in a number of experiments[11,12,22−26] taking advantage of the different selection rules of one- and two-photon absorption spectroscopies for planar macrocycles with D_{2h} symmetry.[27] In the gas phase spectrum of unsubstituted porphyrin the broad absorption features at 4.25, 4.67, and 5.50 eV, known as L (the first two) and M bands,[28] were correlated to B_{3u} and B_{2u} $\pi\pi^*$ states.[22] The nature of these states in terms of excited configurations has been discussed on the basis of accurate ab initio calculations using different theoretical approaches.[29−36] On the contrary, the nearly monotonic increase of the two-photon cross section in tetraphenylporphyrin above the Soret band was attributed to two-photon allowed *g* states,[22] in reasonable agreement with predictions about a series of *g* parity states in the range 3.5−4.5 eV.[37] $Q_x \rightarrow S_n$ absorption of gerade nature, approximately at energies 2.5−2.9 eV above Q_x, shows also in the transient spectrum of octaethyl- and tetraphenylporphyrin.[11] More recently, *g* states of free base tetratolylporphyrin have been observed in the region of the Soret band exciting into the Q_x;Q_y bands and probing with near-infrared pulses.[38]

Following these considerations, in this paper we wish to provide additional information on excited states of porphyrin macrocycles investigating on two systems, diprotonated porphyrin and tetraoxaporphyrin dication (see Figure 1, **2** and **3**, respectively), which are isoelectronic with porphyrin (**1** in Figure 1) and whose structures present interesting differences with respect to **1**, i.e., distortion from planarity in the first case and replacement of inner nitrogen atoms and N−H groups with oxygens in the second. Ruffled and saddled nonplanar conformations[39−41] are well-known macrocycle geometries of several porphyrin-type cofactors of proteins.[42−44] Thus, distorted por-

* To whom correspondence should be addressed. E-mail: piero.salvi@unifi.it.

† Also at Laboratorio Europeo di Spettroscopie non Lineari (LENS), Università di Firenze, via N. Carrara 1, 50019 Sesto Fiorentino, Firenze, Italy and INOA-CNR, Largo E. Fermi 6, 50125 Firenze, Italy.

10.1021/jp803249d CCC: $40.75
Published on Web 10/15/2008

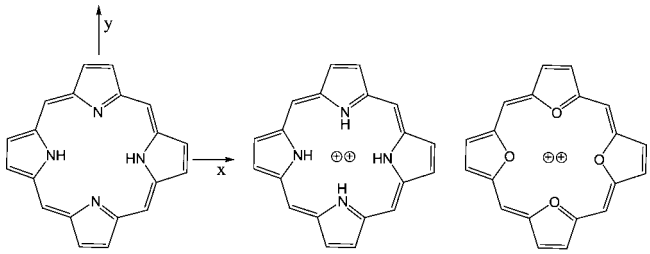

1 2 3

Figure 1. Molecular structures of porphyrin **1**, diprotonated porphyrin **2**, and tetraoxaporphyrin dication **3**. The reference system, common to the three species, is shown for convenience on **1**.

phyrins constitute basic structural units to study the biological effects of conformational flexibility in terms of reduced fluorescence lifetimes and quantum yields and of perturbed excited-state energetics with respect to the neutral planar species.[45−48] Computational results on the diprotonated porphyrin[49−51] indicate that the lowest energy conformer of **2** in the ground-state is nonplanar, saddle-shaped with D_{2d} symmetry because of the steric hindrance between the four hydrogen atoms of the N−H groups. Tetraoxaporphyrin dication has on the contrary a highly symmetrical planar D_{4h} structure.[51−53] For both molecules ground and excited-state absorption spectroscopies give information on states of different symmetry species.[27] In fact, starting from the ground-state the final one-photon active states of $\pi\pi^*$ character are doubly degenerate, of E/E_u symmetry for **2**/**3**. Conversely, in a experiment with Q(E/E_u) as initial state $\pi\pi^*$ states of A_1, A_2, B_1, and B_2 symmetry are reached in the case of **2** and of A_{1g}, A_{2g}, B_{1g}, and B_{2g} symmetry in the case of **3**.

The purpose of the present paper is therefore 2-fold. First, experimental data are reported on excited states of **1**−**3** not available from conventional $S_0 \rightarrow S_n$ spectroscopy. Second, computational results on these states, which have been obtained performing large scale density functional calculations of configuration interaction between singly excited configurations (DF/SCI),[54] are discussed. These calculations complement the information so far provided[29−36,50] on the excited states of **1** and **2** and represent a further attempt to characterize the excited states of **3**.[55]

II. Experimental Section

The chemical preparation of **2** and sample processing for **1**−**3** have been described elsewhere.[51,56] $S_0 \rightarrow S_n$ spectra of **1** (from Frontier Scientific, USA; used as received; benzene/cyclohexane (1:10) solution), of **2** (prepared adding trifluoroacetic acid to the benzene/cyclohexane (1:10) solution of **1**), and of **3** (received as perchlorate salt from Prof. Vogel, University of Koln, Germany) in concentrated $HClO_4$ were measured on a Cary 5 spectrophotometer at room temperature. The solution concentrations were in the range $10^{-4}-10^{-5}$ M. Also, as reported in the synthetic study,[52] the solvent choice for **3** was dictated by the fact that the perchlorate salt has good solubility in strong mineral acids while decomposes in water.

Excited state spectra were measured with the excitation/probe technique using the transient absorption instrumentation assembled in our laboratory.[57] Pulses of ≈100 fs duration and 500 μ J energy are generated at 800 nm by a Ti:sapphire laser system at 1 KHz repetition rate and regeneratively amplified. Excitation pulses of approximately equal time duration and ≈0.8 μ J energy are emitted either at 400 nm doubling the fundamental or at 370 nm thanks to the fourth harmonic of the 1480 nm pulse which is in turn generated by parametric amplification pumping a BBO crystal with the fundamental beam. Spectrally broad pulses ("white continuum") are produced focusing a small portion of the fundamental into a thin CaF_2 crystal. The white continuum beam is divided by a 50:50 beamsplitter into two components of equal intensity, probe and reference. Excitation and probe + reference beams enter the sample, kept under constant stirring in a 2 mm quartz cell, by means of a parabolic mirror in order to minimize spherical and chromatic aberrations. The diameter of the excitation beam before the parabola is half the probe diameter so that the probe overlaps completely the excitation beam inside the sample in an almost collinear arrangement. The original 1 KHz repetition rate is reduced to 100 Hz by means of a synchronized chopper in order to minimize heating effects of the solution. As the probe reaches the sample at delay time τ after excitation, the transient transmittance is measured at any wavelength λ as $T(\tau,\lambda) = I(\tau,\lambda)/I_0(\lambda)$ where $I(\tau,\lambda)$ and $I_0(\lambda)$ are the transmitted intensities of the probe beam with and without the excitation pulse. In order to measure weak transient signals the instrumental sensitivity must be high, i.e., the excitation and probe pulses stable as much as possible. The excitation beam has typical pulse-to-pulse intensity fluctuations of about 0.5%, compensated by averaging over several hundreds shots, usually 500. Fluctuations of the white continuum are more difficult to deal with since they are related not only to the overall pulse intensity but also to the relative intensity of the different spectral components. To this purpose two measurements are performed, taking advantage of the fact that the reference pulse enters temporally the sample before excitation. In the first, with probe + reference beams only, $I_0(\lambda)$ and $I_r(\lambda)$ intensities are acquired while in the second, with both excitation and probe + reference beams, $I(\tau,\lambda)$ and $I_r(\lambda)$. The transient transmittance may be therefore expressed as $[I(\tau,\lambda)/I_r(\lambda)][I_r(\lambda)/I_0(\lambda)]$ and the transient absorbance ΔA as $[1 - T(\tau,\lambda)]/2.303$ in the limit of small variations of $T(\tau,\lambda)$. We have frequently checked the baseline stability $I_r(\lambda)/I_0(\lambda)$ and observed that three runs of 500 shots each give an essentially flat baseline with a resolution in ΔA of ± 0.001 over the spectral range 400−650 nm. The detection system for this measurement as well as for our transient absorption experiments consists of a flat-field spectrometer and a back-illuminated 1100 × 330 CCD camera having optimum spectral response in the range 400−650 nm.

III. Results

$S_0 \rightarrow S_n$ Absorption. The absorption spectra of **1**−**3** in the region of the highly excited $\pi\pi^*$ states, i.e., beyond (and including) the Soret band, are shown in Figure 2. The Q_x,Q_y and Soret bands of **1** have known oscillator strengths.[29] As to **2** and **3**, the oscillator strengths (f) of the Q and B bands have been redetermined with respect to previous data.[56] Since f of strongly allowed transitions[28] is ≈1, the $f = 1.2$ value for the B band of **3** has been related to additional intensity contributions, for instance absorption of close lying g states through vibronic mixing with B. The oscillator strengths of the weak bands above Soret were determined by fitting with Voigt profiles the spectrum expressed as a function of wavenumber. The results are reported in Tables 1−3.

Considering first the dicationic species **3**, two weak bands are observed at 4.10 and 4.48 eV with oscillator strengths 0.05 and 0.02, respectively, that is only few percent the Soret strength. The large intensity difference may be justified recurring to the cyclic polyene model and to the associated selection rule, as it has been proposed since longtime for the intensity ratio between

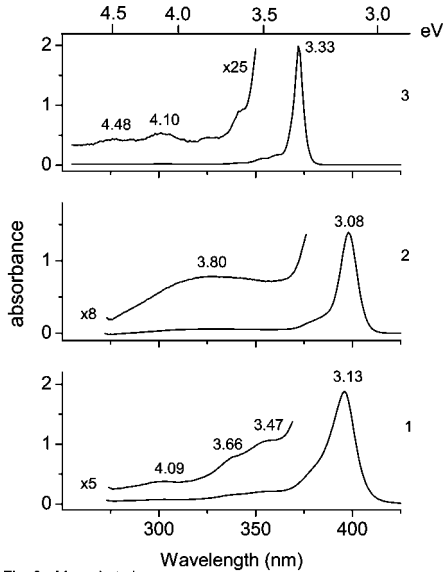

Figure 2. Absorption spectra of **1**−**3** solutions ($c = 4 \times 10^{-5}$, 1.7×10^{-5}, 10^{-5} M, respectively) in the region above (and including) the Soret band at room temperature. Solvents: benzene/cyclohexane for **1**, benzene/cyclohexane and trifluoroacetic acid (5% volume) for **2** and concentrated $HClO_4$ for **3**.

visible and Soret absorption in porphyrins.[28,58] In fact, considering the macrocycle as a circular ring, one-photon transitions are allowed only if the angular momentum about the axis of the ring changes by just one unit, i.e., only promoting one electron between the appropriate components of the doubly degenerate HOMO and LUMO orbitals.[28] Qualitatively, this agrees with the occurrence of one absorption band almost 2 orders of magnitude stronger than all others. In striking contrast, the corresponding absorption of **2** consists of a broad and unstructured band centered around 3.80 eV and extended from ≈ 3.35 eV to ≈ 4.50 eV with oscillator strength 0.35, comparable, though smaller, to that of the Soret band. Additional comments are relative to the neutral species **1**. The Soret peak observed at 3.33 eV in the spectrum of the gaseous molecule[22] shifts to 3.13 eV in the solution phase. Similarly, the weak band with maximum at 4.25 eV in the gas phase shifts to 4.09 eV in solution. Two bands, observed in our spectrum at 3.47 and 3.66 eV, have probably as gas phase counterpart the 3.65 eV shoulder,[22] identified as N band.[58] Gas and solution data are summarized in Tables 1-3.

B. $Q_x \rightarrow S_n$ Absorption. The molecules **1**−**3** are excited in the Soret band (400 nm, **1** and **2**; 370 nm, **3**) and probed at delay times as large as 1.5 ns. With excitation energy ≈ 0.8 μ J/pulse, corresponding to a power density of ≈50 GW/cm^2, no multiphoton process is observed, as it results from the linear dependence of the transient signal on the excitation intensity at half and 1/4 the original intensity. In fact, it has been reported[11] that two-photon absorption contributes to transient signal in porphyrins and metalloporphyrins at power densities three times 100 GW/cm^2. Thus, under our excitation conditions direct two-photon absorption is safely excluded. The observed transient spectrum of **1** after a delay time of 1.5 ns is shown in Figure 3. Since the Q_x lifetime is much longer than 1.5 ns[59] while the relaxation processes to the S_1 origin, including vibrational cooling and solvent rearrangement, are completed within few tens of picoseconds,[16] Q_x is steadily populated in the time regime of the first few nanoseconds and the ground-state depleted. The spectrum has been therefore assigned not only to vertical $Q_x \rightarrow S_n$ transitions starting from the (0−0) level of the Q_x state but in addition to the ground-state bleach, which shows prominently in the region of the Q_x and Q_y bands, between 600 and 475 nm, and more weakly at the onset of the Soret band, below 410 nm. The bleach allows a direct estimate of the number of molecules promoted and relaxed to the Q_x state, ≈25% of the total number of molecules when the comparison is made between transient and static absorbances at the maximum of the Q_y bleach, 486 nm. Since the ground-state concentration of our porphyrin solution is 4×10^{-5} M, the detection capability of the experimental setup in terms of absorption coefficient has been estimated to be ≥500 M^{-1} cm^{-1} with a cell thickness of 2 mm. Comparing the bleach signal at 486 nm with the transient signal at 410 nm (see trace ESA + B in Figure 3) the excited-state extinction coefficient at 410 nm has been estimated ≈2×10^4 M^{-1} cm^{-1}, being 1.5×10^4 M^{-1} cm^{-1} at 486 nm.[59] The $Q_x \rightarrow S_n$ absorption above 420 nm has been resolved comparing the transient spectrum measured at 1.5 ns with the static $S_0 \rightarrow S_n$ spectrum, as indicated in Figure 3. This procedure has been applied also to the transient spectra of **2** and **3** where the ground-state bleach is equally evident.[16] The $Q_x \rightarrow S_n$ spectra, collected in Figure 4, show absorbance signals significantly above the estimated uncertainty ±0.001. For convenience, the baseline of the transient spectrum of **1** has been reported in the Figure.

No band of sizable intensity is observed for porphyrin between ≈2−3 eV above the Q_x origin. Two weak transient bands are seen on a smoothly rising background intensity, roughly centered 2.58 and 2.72 eV above Q_x. A third broadband occurs with maximum tentatively located around 2.25 eV. Also, the increasing absorbance beyond 3 eV suggests the occurrence of a transient band at higher energy. This band however could not be observed due to the combination of reduced white continuum intensity with Soret bleach whose result is a series of progressively noisy transient signals in the 3 eV region. On the contrary, the dicationic species **2** and **3** exhibit intense and well resolved peaks at 2.82 eV, as to **2**, and at 2.90; 3.07 eV, as to **3**, above the respective Q origins, being these energy maxima sufficiently far from the Soret bleach. An additional weak band of **3** is at ≈2.60 eV. The bleaching intensities of the transient spectra[16] have been useful as internal references to estimate excited-state extinction coefficients and oscillator strengths. From the transient absorbances[16] and the ground-state extinction at the bleach wavelength,[59] the coefficient of the transient band of **2** was estimated ≈ 6.2×10^4 M^{-1} cm^{-1}. Applying the same procedure to **3**, the transient coefficients at 2.90 and 3.07 eV are 5.6×10^4 and 3.1×10^4 M^{-1} cm^{-1}, respectively. These values are consistent with those measured in the linear excitation regime.[11] Provided that no decay channel other than the B → Q internal conversion is effective for the relaxation dynamics of **2** and **3**,[16,18] the same number of particles is responsible of the bleaching and of the excited-state contribution to the transient spectrum. The $f_{Q \rightarrow S_n}$ strengths have been obtained from $f_{S_0 \rightarrow Q}$ times the ratio of excited-state intensities to bleaching intensities. The calculated values are 0.13 for the transient band of **2** and 0.10 for each component of the **3** pair. All the spectral data on the transient absorption of **1**−**3** are collected in Table 4.

IV. Discussion

Ab initio density functional calculations of vertical $S_0 \rightarrow S_n$ excitation energies were performed within the singly excited configuration interaction scheme (DF/SCI) by means of the Gaussian 03 suite of programs[60] using the B3-LYP exchange-correlation functional and the cc-pVDZ basis set. The excitation energies of **1**−**3** were calculated promoting electrons from

TABLE 1: Vertical $S_0 \rightarrow S_n$ Excitation Energies and Oscillator Strengths (ΔE, eV; f) of Free Base Porphyrin 1 to the Lowest Excited States, $\pi\pi^*$ unless Otherwise Specified[b]

Exp				DF/SCI			TD/DFT		CASPT2	
gas		sol								
ΔE		ΔE	f	ΔE	f	ass.	ΔE	f	ΔE	f
1.98	Q_x	2.01	0.02[(a)]	2.26	$< 10^{-4}$	$1B_{3u}$	2.24	0.0002	1.63	0.0004
2.42	Q_y	2.38	0.07[(a)]	2.41	$< 10^{-4}$	$1B_{2u}$	2.39	0.00004	2.11	0.002
3.33	B_x;B_y	3.13	1.15[(a)]	3.30	0.42	$2B_{3u}$	3.27	0.40	3.08	0.91
				3.47	0.63	$2B_{2u}$	3.45	0.61	3.12	0.70
				3.39	–	$1B_{1g}$				
				3.57	–	$2A_g$				
3.65	N	3.47	0.19	3.73	0.51	$3B_{2u}$	3.70	0.55	3.42	0.46
		3.66	0.14	3.83	0.78	$3B_{3u}$	3.79	0.82	3.53	0.83
				4.01	–	$2B_{1g}$				
				4.03	–	$1A_u(n\pi^*)$				
				4.05	–	$1B_{2g}(n\pi^*)$				
				4.09	0.001	$1B_{1u}(n\pi^*)$				
				4.09	–	$1B_{3g}(n\pi^*)$				
				4.22	–	$3B_{1g}$				
				4.23	–	$3A_g$				
4.25	L_y	4.09	0.17	4.33	0.12	$4B_{2u}$	4.29	0.12	3.96(L_y)	0.34
									4.04(L_x)	0.20
				4.41	–	$4A_g$				
4.65	L_x			4.44	0.11	$4B_{3u}$	4.40	0.11		
				4.65	–	$4B_{1g}$				
				4.80	–	$5A_g$				
5.50	M			5.14	0.14	$5B_{3u}$				

[a] From ref 29, the 1.15 value corresponds to the sum of the oscillator strengths of the two states. [b] Exp: gas-phase data from ref 22 and our solution data. Calculated values under all other headings: DF/SCI, our results and assignment (reference system as in Figure 1); TD/DFT, results from ref 35; CASPT2, results from ref 34.

valence orbitals (57 in the three cases) to all virtual orbitals (325, 335, and 315 for **1**−**3**, respectively). The ground-state equilibrium geometries, which are the reference structures of the energy calculations, have been determined for **1** and **3** with the same ab initio procedure[51] and found in excellent agreement with X-ray diffraction data on these species.[52,61] The two molecular structures belong to D_{2h} and D_{4h} symmetry groups, respectively. The reference geometry of **2** is the saddled conformation of D_{2d} symmetry[51] whose occurrence has been reported[62] for its tetramethyl and tetraphenyl derivatives. The saddle-shaped conformer is more stable than the second conformer, a quasi-wave C_i structure, by ≈0.22 eV according to calculations.[50,51]

As a preliminary check of the quality of our computational approach, the excitation energies of **1** are presented in Table 1 and compared with experiment and results from recent computational studies.[34,35] It is easily verified that an overall agreement occurs among these calculations from which the assignment of the observed $S_0 \rightarrow S_n$ bands higher than Soret is derived. The $3B_{3u}/3B_{2u}$ pair of states calculated at 3.83 and 3.73 eV correspond to the unresolved gas phase N band at 3.65 eV and to the N_x/N_y pair of solution bands at 3.47 and 3.66 eV. The gas phase bands observed at 4.25 and 4.65 eV and denoted L_y and L_x are assigned to the $4B_{2u}$ and $4B_{3u}$ states with calculated excitation energies 4.33 and 4.44 eV.

In Table 4 the assignment of the transient spectrum is proposed in terms of vertical excitation energies from $(0-0)Q_x$ to states of g symmetry. Adding to the transient bands of **1** the Q_x-S_0 energy gap,[56] 2.01 eV, excited-state levels are found at 4.73, 4.59, and 4.26 eV above S_0. Due to non adiabaticity, these excitation energies, associated with the Q_x equilibrium geometry, are in principle different from those calculated ab initio, which refer to the ground-state geometry. However, the absence of strong progressions in the absorption and fluorescence spectra[63,64] and the small Stokes shift between the two spectra[56] support the view that the equilibrium geometry does not undergo a large difference going from the ground to the Q_x state.[65] The calculated $S_0 \rightarrow S_n$ energies may be considered sufficiently accurate for a discussion of the transient spectrum. As a second point, it is evident that close-lying bands, such as those falling at 2.58 and 2.72 eV, could be assigned either to different electronic states or, alternatively, to a single state, the second band as a vibronic addition to the first. This difficulty indicates the degree of uncertainty encountered in the assignment of the upper excited states probed by transient absorption. Table 1 shows that the vertical excitation energies to $4B_{1g}$ and $5A_g$,

TABLE 2: Vertical $S_0 \rightarrow S_n$ Excitation Energies and Oscillator Strengths (ΔE, eV; f), of Diprotonated Porphyrin 2[a]

Exp		PH_4^{2+}			$PH_4^{2+}(HCOO^-)_2$		
ΔE	f	ΔE	f	Assign.; main config.	ΔE	f	Assign.; main config.
2.08	0.032	2.29	0.0005	1E; $12b_2 \rightarrow 21e$, $9b_1 \rightarrow 21e$	2.10	0.003	1E;$18b_2 \rightarrow 26e$, $10b_1 \rightarrow 26e$
					2.57	0.017	2E; $17b_2 \rightarrow 26e$, CT
					2.61	0.005	3E; $19a_1 \rightarrow 26e$, CT
					2.637	0.	$1A_2$; $25e \rightarrow 26e$
					2.638	0.	$1B_1$; $25e \rightarrow 26e$
					2.643	0.	$2A_1$; $25e \rightarrow 26e$
					2.644	0.007	$1B_2$; $25e \rightarrow 26e$
					2.86	0.002	4E; $8a_2 \rightarrow 26e$, $9b_1 \rightarrow 26e$, CT
					2.90	0.004	5E; $8a_2 \rightarrow 26e$, $9b_1 \rightarrow 26e$, CT
3.08	0.8	3.59	1.25	2E; $12b_2 \rightarrow 21e$, $9b_1 \rightarrow 21e$	3.33	0.68	6E;$18b_2 \rightarrow 26e$, $10b_1 \rightarrow 26e$
		3.839	0.	$1A_2$; $20e \rightarrow 21e$			
					3.69	0.	$2B_1$; $18b_2 \rightarrow 9a_2$
		3.843	0.	$1B_1$; $20e \rightarrow 21e$			
					3.73	0.	$2A_2$; $24e \rightarrow 26e$
					3.80	0.	$3B_1$; $18b_2 \rightarrow 9a_2$
		3.96	0.001	$1B_2$; $20e \rightarrow 21e$,$9b_1 \rightarrow 8a_2$			
					3.87	0.0007	$2B_2$; $24e \rightarrow 26e$
					3.94	0.	$3A_1$; $24e \rightarrow 26e$
		3.98	0.	$2A_1$; $20e \rightarrow 21e$			
3.80	0.35	3.86	0.003	$3E; 13a_1 \rightarrow 21e$	3.95	0.25	$7E; 16b_2 \rightarrow 26e, 18a_1 \rightarrow 26e$
		4.03	0.07	$4E; 11b_2 \rightarrow 21e$	4.01	0.08	$8E; 16b_2 \rightarrow 26e, 18a_1 \rightarrow 26e$
		4.423	0.	$2B_1$; $12b_2 \rightarrow 8a_2$			
					4.11	0.008	$3B_2$; $10b_1 \rightarrow 9a_2$
		4.424	0.003	$2B_2$; $9b_1 \rightarrow 8a_2$			
					4.27	0.	$3A_2$; $19a_1 \rightarrow 9a_2$, CT
		4.46	0.	$2A_2$; $19e \rightarrow 21e$			
					4.30	0.004	9E; $25e \rightarrow 9a_2$

[a] Exp: solution data. PH_4^{2+} and PH_4^{2+} $(HCOO^-)_2$ headings: calculated DF/B3-LYP/cc-pVDZ/SCI values of ΔE and f with assignment (see Figure 5 for MO labels). CT indicates excited states of PH_4^{2+} $(HCOO^-)_2$ with charge transfer character.

calculated at 4.65 and 4.80 eV, satisfactorily match the transient bands observed at 4.59 and 4.73 eV, a result clearly in favor of the first choice, though not conclusive. On the other hand, the transient band at 4.26 eV, quite far from the two above-mentioned, is assigned to either $3B_{1g}$ or $3A_g$ (or both), the two states being calculated almost accidentally degenerate at 4.22 and 4.23 eV. The comparison with the transient data on the tetratolyl derivative of porphyrin[38] is also rewarding. Allowed $Q_x \rightarrow S_n$ transitions have been reported at 2.80, 3.2−3.25 eV and >3.7 eV, i.e., 0.16 eV below and 0.24−0.29 eV and >0.74 eV above the Soret band at 2.96 eV and correlated with g states of porphyrin.[38] In the DF/SCI calculation on the free base vertical excitation energies to the lowest g states, $1B_{1g}$, $2A_g$, and $2B_{1g}$, are predicted at 3.39, 3.57, and 4.01 eV. The energy spacings with respect to the average value of the Soret doublet (B_{3u}, 3.30 eV; B_{2u}, 3.47 eV; see Table 1) are not far from those observed on tetratolylporphyrin.

A. Excited States of Tetraoxaporphyrin Dication. Let us consider now tetraoxaporphyrin **3**. In D_{4h} symmetry excited $\pi\pi^*$ states behave symmetrically under reflection with respect to the molecular plane and therefore belong to A_{1g}, A_{2g}, B_{1g}, B_{2g}, and E_u species. The only states showing one-photon $S_0 \rightarrow S_n$ activity are those of E_u character among which Q and B are included. The vertical excitation energies $S_0 \rightarrow S_n$ (E_u) ($n = 1, ..., 4$) calculated at 2.34, 3.75, 4.28, and 4.56 eV fit satisfactorily the experimental values on **3**, as shown in Table 3, and are in good agreement with recent results.[55] The calculation describes these states in terms of linear combinations of a relatively small number of singly excited configurations. In the MO energy diagram of Figure 5 the two top filled π orbitals, HOMO and HOMO − 1, are quasi degenerate and classified as $3a_{2u}$ and $1a_{1u}$ while LUMO and LUMO + 1 are the doubly degenerate orbitals $4e_{g,a}$ and $4e_{g,b}$, respectively, whose nodal properties have been already examined.[66,67] According to our results, the Q and B states are mainly represented by means of the four excited configurations $3a_{2u}^1\ 4e_{g,a}^1$, $1a_{1u}^1\ 4e_{g,b}^1$, $3a_{2u}^1\ 4e_{g,b}^1$, and $1a_{1u}^1\ 4e_{g,a}^1$. For instance, the x components of the doubly degenerate B and Q states are $(3a_{2u}^1\ 4e_{g,b}^1 \pm 1a_{1u}^1\ 4e_{g,a}^1)$, respectively. Since the

TABLE 3: Vertical $S_0 \rightarrow S_n$ Excitation Energies and Oscillator Strengths (ΔE, eV; f) of Tetraoxaporphyrin Dication 3 to the Lowest $\pi\pi^*$ Excited States[a]

exp		calc		
ΔE	f	ΔE	f	assign.; main config.
2.17	0.042	2.34	0.0005	$1E_u$; $3a_{2u} \rightarrow 4e_g$, $1a_{1u} \rightarrow 4e_g$
3.33	1.2	3.75	1.56	$2E_u$; $3a_{2u} \rightarrow 4e_g$, $1a_{1u} \rightarrow 4e_g$
		4.14	0	$1A_{2g}$; $3e_g \rightarrow 4e_g$
		4.21	0	$2A_{1g}$; $3e_g \rightarrow 4e_g$
		4.24	0	$1B_{2g}$; $3e_g \rightarrow 4e_g$
4.10	0.05	4.28	0.027	$3E_u$; $2b_{2u} \rightarrow 4e_g$
		4.28	0	$1B_{1g}$; $3e_g \rightarrow 4e_g$, $1a_{1u} \rightarrow 2b_{1u}$
4.48	0.02	4.56	0.0004	$4E_u$; $2a_{2u} \rightarrow 4e_g$
		4.63	0	$2B_{2g}$; $2a_{2u} \rightarrow 2b_{1u}$
		4.636	0	$2B_{1g}$; $2a_{1u} \rightarrow 2b_{1u}$
		4.75	0	$2A_{2g}$; $2e_g \rightarrow 4e_g$
		4.97	0	$3A_{1g}$; $2e_g \rightarrow 4e_g$
		4.98	0	$3B_{1g}$; $3a_{2u} \rightarrow 3b_{2u}$, $2e_g \rightarrow 4e_g$
		5.09	0	$3B_{2g}$; $1a_{1u} \rightarrow 3b_{2u}$, $2e_g \rightarrow 4e_g$
		5.80	0.0002	$5E_u$; $1b_{1u} \rightarrow 4e_g$
		5.82	0	$4B_{2g}$; $1a_{1u} \rightarrow 3b_{2u}$
		5.88	0	$4B_{1g}$; $3a_{2u} \rightarrow 3b_{2u}$

[a] Exp: solution data. Calc: DF/B3-LYP/cc-pVDZ/SCI results and assignment. With reference to Figure 5, the most significant configurations contributing to excited states are detailed.

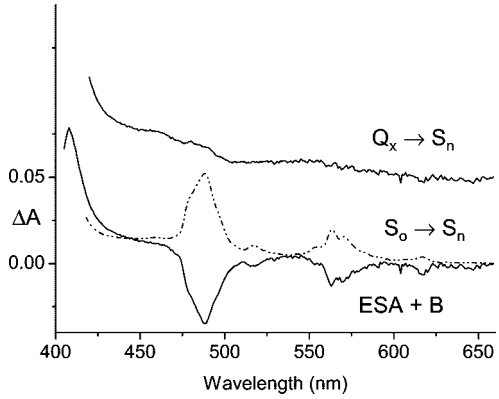

Figure 3. Transient spectrum of **1** experimentally observed at 1.5 ns delay time (ESA + B), from which the static $S_0 \rightarrow S_n$ spectrum is subtracted, gives as a result the $Q_x \rightarrow S_n$ spectrum.

transition moments from S_0 to the $3a^1_{2u}\ 4e^1_{g,b}$ and $1a^1_{1u}\ 4e^1_{g,a}$ configurations are large and almost equal, these moments add constructively for the B state and destructively for the Q state, making the two intensities strongly different. Of course, an analogous result holds for the *y* components of the same states. Due to the increased energy gap between the $2b_{2u}$ and $2a_{2u}$ orbitals, which are HOMO − 5 and HOMO − 6 in Figure 5, the next two states, $3E_u$ and $4E_u$, are approximately represented by the configurations $2b^1_{2u}\ 4e^1_{g,b}$ and $2a^1_{2u}\ 4e^1_{g,b}$, as to the *x* component, and by $2b^1_{2u}\ 4e^1_{g,a}$ and $2a^1_{2u}\ 4e^1_{g,a}$, as to the *y* component. The oscillator strengths of the $S_0 \rightarrow S_3$ (E_u) and $S_0 \rightarrow S_4$ (E_u) transitions are calculated much weaker than that of the B state, as observed.

Going to the transient $Q \rightarrow S_n$ spectrum, A_{1g}, A_{2g}, B_{1g}, and B_{2g} $\pi\pi^*$ states are responsible of the observed activity. Our DF/SCI results indicate that several states of *g* symmetry occur between 4.10 and 4.30 eV and between 4.60 and 5.10 eV above S_0. The next *g* states are predicted at 5.82 and 5.88 eV with a wide gap with respect to the previous states. The transient spectrum of Figure 4, with absorption bands at 5.07 and 5.14 eV once the $Q-S_0$ energy gap of 2.17 eV[56] is taken into account, is in reasonable agreement with *g* states in the range 4.60−5.10

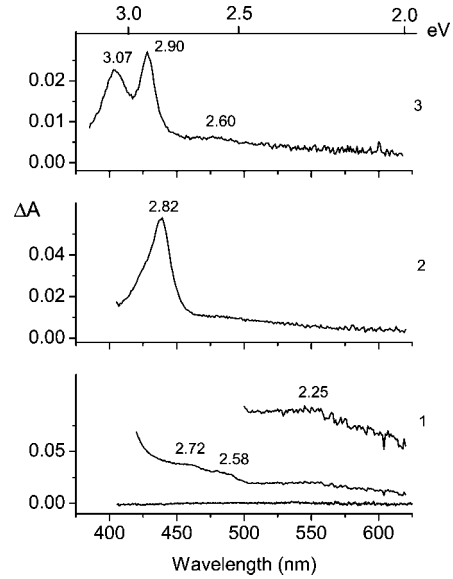

Figure 4. $Q_x/Q \rightarrow S_n$ absorption spectra of **1** −**3** solutions ($c = 4 \times 10^{-5}$, 1.7×10^{-5}, 10^{-5} M, respectively) in the region 2−3 eV above the lowest excited state (Q_x for **1** and Q for **2** and **3**) observed after 1.5 ns delay. The femtosecond pulse excites **1** and **2** at 400 nm and **3** at 370 nm. The baseline trace is shown along with the spectrum of porphyrin.

TABLE 4: $Q_x \rightarrow S_n$ Transient Spectrum of 1 (Left) and Q $\rightarrow S_n$ Transient Spectra of 2 and 3 (Right) in the 2−3 eV Region[c]

1			3			
obs	calc		obs		calc	
$\Delta E^{(a)}$	ΔE	Assign.	$\Delta E^{(a)}$	$f_{Q \rightarrow S_n}$	ΔE	Assign.
4.26 (2.25)	4.22	$3B_{1g}$	4.77 (2.60)		4.75	$2A_{2g}$
	4.23	$3A_g$				
4.59 (2.58)	4.65	$4B_{1g}$	5.07 (2.90)	0.10	4.97	$3A_{1g}$
					4.98	$3B_{1g}$
4.73 (2.72)	4.80	$5A_g$	5.14 (3.07)	0.10	5.09	$3B_{2g}$
			2			
			obs		calc[(b)]	
			4.90 (2.82)	0.13	4.83	$5B_2$

[a] The Q_x/Q origins of **1** and **3** have been reported at 2.01 and 2.17 eV while the origin of **2** has been estimated at 2.08 eV (see Tables 1−3 and ref 56). [b] Vertical excitation energy calculated for the diprotonated porphyrin complex with the formiate anion. Other excitation energies of the complex calculated in this energy region are at 4.57 eV ($5A_1$), 4.57 eV ($4B_2$), 4.95 eV ($5B_1$), 5.21 eV ($6B_2$). [c] The excitation energies with respect to S_0 (ΔE, eV) and excited state oscillator strengths $f_{Q \rightarrow S_n}$ are reported; in parentheses the experimentally observed excitation energies as shown in Figure 4. The spectral assignment follows from calculation data of Tables 1−3.

eV, i.e., $3A_{1g}$, $3B_{1g}$, and $3B_{2g}$, as proposed in Table 4. It should be reminded, however, that in absence of more information the assignment of the two bands to only one of these states with one vibronic addition cannot be excluded.

B. Excited States of Diprotonated Porphyrin. Above the Soret band the absorption spectrum shows a single broad and relatively intense band centered at 3.80 eV in place of the weak and structured profiles of **1** and **3**. The calculated excitation energies of **2** in D_{2d} symmetry match reasonably the observed values while the oscillator strengths of the $S_0 \rightarrow 3E$ and $S_0 \rightarrow 4E$ transitions are exceedingly small, as it is seen from Table

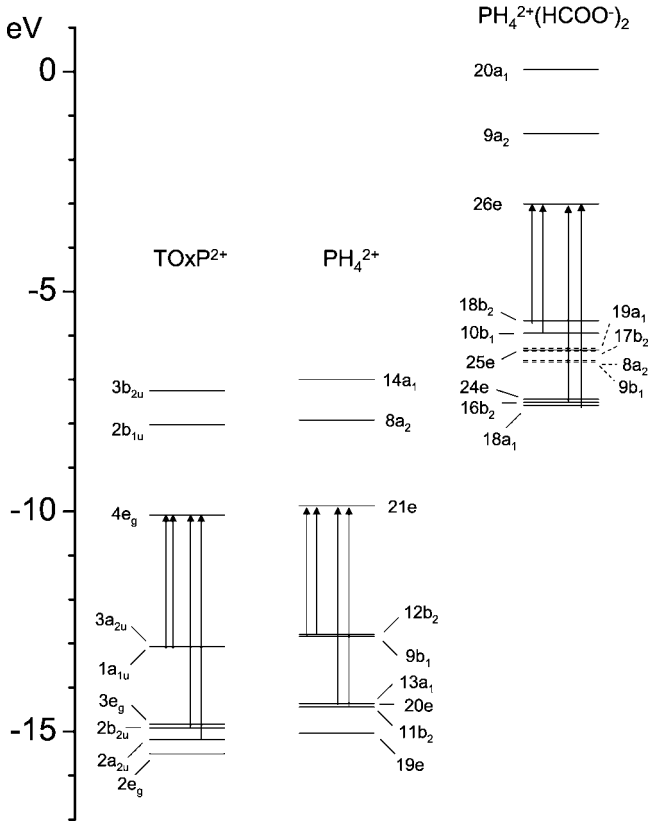

Figure 5. Energy diagram showing the highest occupied and lowest virtual molecular orbitals of tetraoxaporphyrin dication ($TOxP^{2+}$), of diprotonated porphyrin (PH_4^{2+}) and of the complex with the formiate anion [$PH_4^{2+}(HCOO^-)_2$]. The molecular orbitals are classified according to the D_{4h} and D_{2d} molecular symmetries of $TOxP^{2+}$ and PH_4^{2+}, $PH_4^{2+}(HCOO^-)_2$, respectively. Dashed energy levels along the $PH_4^{2+}(HCOO^-)_2$ diagram are relative to molecular orbitals of the complex mostly located on the formiate anion. Vertical arrows indicate singly excited configurations contributing to one-photon $S_0 \rightarrow S_n$ absorption.

2. Following the indications of studies on the decay kinetics of diprotonated porphyrin derivatives[49,68] and of **2**,[16,56] here it is proposed that the discrepancy depends on the occurrence in solution of a species closely related but different from **2**, i.e., the complex of PH_4^{2+} with the trifluoroacetate anion, $PH_4^{2+}(CF_3COO^-)_2$. The structures of $PH_4^{2+}(CF_3COO^-)_2$ and of the second complex generated by proton transfer, formally $(PH_2)(CF_3COOH)_2$, were optimized. The equilibrium geometries of the two complexes are shown in Figure 6. In the first, the CF_3COO^- counterions along the z axis above and below the PH_4^{2+} ring are bound to the macrocycle, with all the four closest O···H distances between oxygen atoms and hydrogen of the NH groups equal to 1.572 Å. In the second, two hydrogen atoms of adjacent NH groups (one above and one below the average macrocycle plane) migrate approaching the oxygen atoms at 1.024 Å while the other two move away to a distance 2.132 Å. Two equivalent $(PH_2)(CF_3COOH)_2$ structures (A_1 and A_2 in Figure 6) are obtained by simply interchanging the pairs of hydrogens atoms. The $PH_4^{2+}(CF_3COO^-)_2$ structure (B in Figure 6) is therefore the transition state between them with an activation barrier of only 0.05 eV (≈1.2 kcal/mol). As the barrier is easily surmounted at room temperature, the molecular complex may be effectively modeled as one having on the average the symmetrical arrangement of B. For a better correlation between results on the complex and on the isolated macrocycle we decided to retain the D_{2d} symmetry taking into consideration the complex with the formiate anion, $PH_4^{2+}(HCOO^-)_2$. The optimized structure of $PH_4^{2+}(HCOO^-)_2$ is substantially similar to that of $PH_4^{2+}(CF_3COO^-)_2$ with a small decrease of the O···H distance to 1.502 Å.[56] The DF/B3-LYP/cc-pVDZ/SCI calculation has been performed on this complex with a configuration interaction scheme as large as possible, i.e., including all single electronic excitations from valence (75) to virtual (405) orbitals of the complex. The results are reported in Table 2, where the Soret state of the complex is classified as 6E. Two points of our calculation are noteworthy; (i) excited states localized on the macrocycle ($1A_2$, $1B_1$, $1B_2$, and $2A_1$) as well as CT states (2E,..., 5E) fall in the energy range between 1E and 6E contributing through internal conversion to the non radiative decay from the Soret to the Q state and, for the purpose of the present work, (ii) the $S_0 \rightarrow 7E$ transition has a relatively high oscillator strength at excitation energy close to the observed 3.80 eV maximum. This transition corresponds to the very weak $S_0 \rightarrow 3E$ of the isolated PH_4^{2+} species. The two states, 7E in the case of $PH_4^{2+}(HCOO^-)_2$ and 3E in the case of PH_4^{2+}, are described by excited configurations, $16b_2^1 26e^1$ and $18a_1^1 26e^1$ for the former system and $13a_1^1 21e^1$ and $11b_2^1 21e^1$ for the latter, which may be easily correlated from inspection of the MO energy diagram of Figure 5. From this point of view no substantial difference exists between the two states. However, due to the strong interaction of the macrocycle with the formiate counterions, 7E has also a new significant contribution from CT excitations such as $17b_2^1 26e^1$. The increase of the oscillator strength may thus be attributed to the partial CT character of the 7E state, plausibly causing an appreciable charge displacement during the electronic excitation.

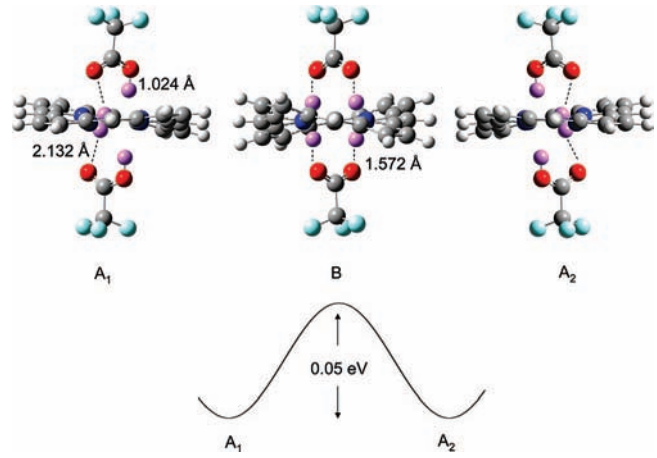

Figure 6. Complex of diprotonated porphyrin with trifluoroacetic acid according to DFT/B3-LYP/cc-pVDZ calculations. A_1, A_2: $(PH_2)(CF_3COOH)_2$ tautomers. B: $(PH_4^{2+})(CF_3COO^-)_2$ transition structure. For the sake of clarity, the four central hydrogen atoms are evidentiated as violet balls for the three structures and their distances (Å) from the closest oxygen atoms are indicated. Bottom: schematic diagram of the potential energy relating A_1 and A_2 through the transition structure B with an energy barrier of 0.05 eV.

V. Conclusions

In this work we have investigated about highly excited states of porphyrin, diprotonated porphyrin and tetraoxaporphyrin dication by means of transient $S_1 \rightarrow S_n$ spectroscopy and reconsidering the $S_0 \rightarrow S_n$ absorption spectrum. The comparison with DF/B3-LYP/cc-pVDZ/SCI calculation results on the three molecular species has allowed to draw the following conclusions:

(1) The lowest $\pi\pi^*$ excited states of porphyrin up to 5.50 eV have been assigned combining one-photon gas-phase[22] and solution data with our transient absorption results as well as with those from a second source.[38]

(2) The $S_0 \rightarrow S_n$ absorption spectrum of tetraoxaporphyrin conforms satisfactorily to the cyclic polyene model and is assigned to the lowest four E_u states of the dication. Transient $S_1 \rightarrow S_n$ bands in the energy range 4.60−5.10 eV above S_0 are due to transitions from S_1 to dark states of *g* symmetry.

(3) The $S_0 \rightarrow S_n$ absorption intensity of **2** above the Soret band has been related to the occurrence in solution of the molecular complex of **2** with the trifluoroacetate anion, for which excited states of charge transfer character are relevant.

Acknowledgment. The authors are grateful to Prof. E. Vogel (University of Köln, Germany) for the generous gift of a sample of tetraoxaporphyrin perchlorate. This work was supported by INSTM under the contract FIRB RBNE033KMA and by the European Community under the contract RIII-CT-2003-506350.

References and Notes

(1) Alberts, B.; Johnson, A.; Lewis, J.; Raff, M.; Walter, P. *Molecular Biology of the Cell*; Garland Science: New York, 2002.
(2) Deisenhofer, J. *The Photosynthetic Reaction Center*; Norris, J. R., Ed.; Academic Press: San Diego, 1993.
(3) *Chlorophylls*; Scheer, H., Ed.; CRC Press: Boca Raton, 1991.
(4) *The Porphyrins*; Dolphin, D., Ed.; Academic Press: New York, 1978; Vols. *I*−*VII*.
(5) Gouterman, M.; Dolphin, D., Ed.; Academic Press: New York, 1978; pp 1−165.
(6) Gouterman, M. *J. Chem. Phys.* **1959**, *30*, 1139.
(7) Even, U.; Magen, J.; Jortner, J.; Friedman, J.; Levanon, H. *J. Chem. Phys.* **1982**, *77*, 4374.
(8) Ponterini, G.; Serpone, N.; Bergkamp, M. A.; Netzel, T. L. *J. Am. Chem. Soc.* **1983**, *105*, 4639.
(9) Aaviksoo, J.; Freiberg, A.; Savikhin, S.; Stelmakh, G. F.; Tsvirko, M. P. *Chem. Phys. Lett.* **1984**, *111*, 275.
(10) Tait, C. D.; Holten, D.; Barley, M. H.; Dolphin, D.; James, B. R. *J. Am. Chem. Soc.* **1985**, *107*, 1930.
(11) Rodriguez, J.; Kirmaier, C.; Holten, D. *J. Am. Chem. Soc.* **1989**, *111*, 6500.
(12) Chosrowjan, H.; Taniguchi, S.; Okada, T.; Takagi, S.; Arai, T.; Tokumaru, K. *Chem. Phys. Lett.* **1995**, *242*, 644.
(13) Vacha, M.; Machida, S.; Horie, K. *J. Phys. Chem.* **1995**, *99*, 13163.
(14) Baskin, J. S.; Yu, H.-Z.; Zewail, A. H. *J. Phys. Chem. A* **2002**, *106*, 9837.
(15) Akimoto, S.; Yamazaki, T.; Yamazaki, I.; Osuka, A. *Chem. Phys. Lett.* **1999**, *309*, 177.
(16) Marcelli, A.; Foggi, P.; Moroni, L.; Gellini, C.; Salvi, P. R. *J. Phys. Chem. A* **2008**, *112*, 1864.
(17) Yu, H.-Z.; Baskin, J. S.; Zewail, A. H. *J. Phys. Chem. A* **2002**, *106*, 9845.
(18) Gurzadyan, G. G.; Tran-Thi, T.-H.; Gustavsson, T. *J. Chem. Phys.* **1998**, *108*, 385.
(19) Gurzadyan, G. G.; Tran-Thi, T.-H.; Gustavsson, T. New Trends in Atomic and Molecular Spectroscopy. Gurzadyan, G. G., Karmenyan, A. V., Eds.; *SPIE*, 2000; *vol. 4060*, pp 96−103.
(20) Dietzek, B.; Maksimenka, R.; Kiefer, W.; Hermann, G.; Popp, J.; Schmitt, M. *Chem. Phys. Lett.* **2005**, *415*, 94.
(21) Sorgues, S.; Poisson, L.; Raffael, K.; Krim, L.; Soep, B.; Shafizadeh, N. *J. Chem. Phys.* **2006**, *124*, 114302.
(22) Edwards, L.; Dolphin, D. H.; Gouterman, M.; Adler, A. D. *J. Mol. Spectry* **1971**, *38*, 16.
(23) Tobita, S.; Kaizu, Y.; Kobayashi, H.; Tanaka, I. *J. Chem. Phys.* **1984**, *81*, 2962.
(24) Aleman, E. A.; Rajesh, C. S.; Ziegler, C. J.; Modarelli, D. A. *J. Phys. Chem. A* **2006**, *110*, 8605.
(25) Drobizhev, M.; Karotki, A.; Kruk, M.; Rebane, A. *Chem. Phys. Lett.* **2002**, *355*, 175.
(26) Kruk, M.; Karotki, A.; Drobizhev, M.; Kuzmitsky, V.; Gael, V.; Rebane, A. *J. Luminesc.* **2003**, *105*, 45.
(27) Klessinger, M.; Michl, J.; *Excited states and photochemistry of organic molecules*; VCH Publishers: New York, 1994.
(28) Murrel, J. N. *Theory of the Electronic Spectra of Organic Molecules*; Methuen: London, 1963.
(29) Nagashima, U.; Takada, T.; Ohno, K. *J. Chem. Phys.* **1986**, *85*, 4524.
(30) Nakatsuji, H.; Hasegawa, J.; Hada, M. *J. Chem. Phys.* **1996**, *104*, 2321.
(31) Nooijen, M.; Bartlett, R. J. *J. Chem. Phys.* **1997**, *106*, 6449.
(32) Gwaltney, S. R.; Bartlett, R. J. *J. Chem. Phys.* **1998**, *108*, 6790.
(33) Tokita, Y.; Hasegawa, J.; Nakatsuji, H. *J. Phys. Chem. A* **1998**, *102*, 1843.
(34) Serrano-Andres, L.; Merchan, M.; Rubio, M.; Roos, B. O. *Chem. Phys. Lett.* **1998**, *295*, 195.
(35) Sundholm, D. *Phys. Chem. Chem. Phys.* **2000**, *2*, 2275.
(36) Parusel, A. B. J.; Ghosh, A. *J. Phys. Chem. A* **2000**, *104*, 2504.
(37) Masthay, M. B.; Findsen, L. A.; Pierce, B. M.; Bocian, D. F.; Lindsey, J. S.; Birge, R. R. *J. Chem. Phys.* **1986**, *84*, 3901.
(38) Schalk, O.; Brands, H.; Balaban, T. S.; Unterreiner, A.-N. *J. Phys. Chem. A* **2008**, *112*, 1719.
(39) Ravikanth, M.; Chandrashekar, T. K. *Struct. Bonding (Berlin)* **1995**, *82*, 105.
(40) Jentzen, W.; et al. *J. Am. Chem. Soc.* **1995**, *117*, 11085.
(41) Nurco, D. J.; Medforth, C. J.; Forsyth, T. P.; Olmstead, M. M.; Smith, K. M. *J. Am. Chem. Soc.* **1996**, *118*, 10918.
(42) Barkigia, K. M.; Chantranupong, L.; Smith, K. M.; Fajer, J. *J. Am. Chem. Soc.* **1988**, *110*, 7566.
(43) Telser, J. *Struct. Bonding (Berlin)* **1998**, *91*, 31.
(44) Wondimagegn, T.; Ghosh, A. *J. Am. Chem. Soc.* **2000**, *122*, 6375.
(45) Gentemann, S.; Medforth, C. J.; Forsyth, T. P.; Nurco, D. J.; Smith, K. M.; Fajer, J.; Holten, D. *J. Am. Chem. Soc.* **1994**, *116*, 7363.
(46) Gentemann, S.; Nelson, N. Y.; Jaquinod, L.; Nurco, D. J.; Leung, S. H.; Medforth, C. J.; Smith, K. M.; Fajer, J.; Holten, D. *J. Phys. Chem. B* **1997**, *101*, 1247.
(47) Shelnutt, J. A.; Song, X. Z.; Ma, J.-G.; Jia, S.-L.; Jentzen, W.; Medforth, C. J. *Chem. Soc. Rev.* **1998**, *27*, 31.
(48) Parusel, A. B. J.; Wondimagegn, T.; Ghosh, A. *J. Am. Chem. Soc.* **2000**, *122*, 6371.
(49) Avilov, I. V.; Panarin, A. Y.; Chirvony, V. S. *Chem. Phys. Lett.* **2004**, *389*, 352.
(50) Chen, D.-M.; Liu, X.; He, T.-J.; Liu, F.-C. *Chem. Phys.* **2003**, *289*, 397.
(51) Jelovica, I.; Moroni, L.; Gellini, C.; Salvi, P. R.; Orlic, N. *J. Phys. Chem. A* **2005**, *109*, 9935.
(52) Vogel, E.; Haas, W.; Knipp, B.; Lex, J.; Schmickler, H. *Angew. Chem., Int. Ed. Engl.* **1988**, *27*, 406.
(53) Malsch, K.; Roeb, M.; Karuth, V.; Hohlneicher, G. *Chem. Phys.* **1998**, *227*, 331.
(54) Grimme, S. *Chem. Phys. Lett.* **1996**, *259*, 128.
(55) Wan, J.; Ren, Y.; Wu, J.; Xu, X. *J. Phys. Chem. A* **2004**, *108*, 9453.
(56) Marcelli, A.; Foggi, P.; Moroni, L.; Gellini, C.; Salvi, P. R.; Badovinac, I. J. *J. Phys. Chem. A* **2007**, *111*, 2276.
(57) Neuwhal, F. V. R.; Bussotti, L.; Foggi, P. *Res. Adv. Photochem. Photobiol.* Global Research Network: Trivandrum, India, 2000; Vol. 1, pp 77−94.
(58) Simpson, W. T. *J. Chem. Phys.* **1949**, *17*, 1218.
(59) Ohno, O.; Kaizu, Y.; Kobayashi, H. *J. Chem. Phys.* **1985**, *82*, 1779.
(60) Frisch, M. J.; Trucks, G. W.; Schlegel, H. B.; Scuseria, G. E.; Robb, M. A.; Cheeseman, J. R.; Montgomery, J. A., Jr.; Vreven, T.; Kudin, K. N.; Burant, J. C.; Millam, J. M.; Iyengar, S. S.; Tomasi, J.; Barone, V.; Mennucci, B.; Cossi, M.; Scalmani, G.; Rega, N.; Petersson, G. A.; Nakatsuji, H.; Hada, M.; Ehara, M.; Toyota, K.; Fukuda, R.; Hasegawa, J.; Ishida, M.; Nakajima, T.; Honda, Y.; Kitao, O.; Nakai, H.; Klene, M.; Li, X.; Knox, J. E.; Hratchian, H. P.; Cross, J. B.; Bakken, V.; Adamo, C.; Jaramillo, J.; Gomperts, R.; Stratmann, R. E.; Yazyev, O.; Austin, A. J.; Cammi, R.; Pomelli, C.; Ochterski, J. W.; Ayala, P. Y.; Morokuma, K.; Voth, G. A.; Salvador, P.; Dannenberg, J. J.; Zakrzewski, V. G.; Dapprich, S.; Daniels, A. D.; Strain, M. C.; Farkas, O.; Malick, D. K.; Rabuck, A. D.; Raghavachari, K.; Foresman, J. B.; Ortiz, J. V.; Cui, Q.; Baboul, A. G.; Clifford, S.; Cioslowski, J.; Stefanov, B. B.; Liu, G.; Liashenko, A.; Piskorz, P.; Komaromi, I.; Martin, R. L.; Fox, D. J.; Keith, T.; Al-Laham, M. A.; Peng, C. Y.; Nanayakkara, A.; Challacombe, M.; Gill, P. M. W.; Johnson, B.; Chen, W.; Wong, M. W.; Gonzalez, C.; Pople, J. A. Gaussian 03, revision B.05; Gaussian, Inc.: Wallingford, CT, 2004.
(61) Chen, B. M. L.; Tulinski, A. J. *J. Am. Chem. Soc.* **1972**, *94*, 4144.
(62) Cheng, B.; Munro, O. Q.; Marques, H. M.; Scheidt, W. R. *J. Am. Chem. Soc.* **1997**, *119*, 10732.
(63) Radziszewski, J. W. J. G.; Michl, J. *J. Mol. Spectrosc.* **1990**, *140*, 373.
(64) Radziszewski, J. G.; Waluk, J.; Nepras, M.; Michl, J. *J. Phys. Chem.* **1991**, *95*, 1963.
(65) Santoro, F.; Lami, A.; Improta, R.; Bloino, J.; Barone, V. *J. Chem. Phys.* **2008**, *128*, 224311.
(66) Longuet-Higgins, H. C.; Rector, C. W.; Platt, J. R. *J. Chem. Phys.* **1950**, *18*, 1174.
(67) Gouterman, M. *J. Mol. Spectrosc.* **1961**, *6*, 138.
(68) Knyukshto, V. N.; Solovyov, K.; Egorova, G. D. *Biospectroscopy* **1998**, *4*, 121.

JP803249D